Limnol. Oceanogr., 46(7), 2001, 1653–1660
© 2001, by the American Society of Limnology and Oceanography, Inc.

Production-respiration relationships at different timescales within the Biosphere 2 coral reef biome

James L. Falter[1]
Department of Oceanography, University of Hawaii at Manoa, 1000 Pope Road, Honolulu, Hawaii 96822

M. J. Atkinson
Hawaii Institute of Marine Biology, Kaneohe, Hawaii 96744; and Biosphere 2 Center, Oracle, Arizona 85623

Chris Langdon
Lamont-Doherty Earth Observatory, Department of Marine Biology, Palisades, New York 10964; and Biosphere 2 Center, Oracle, Arizona 85623

Abstract

Temporal relationships between organic carbon production and respiration are not well understood in coral reef ecosystems. We monitored dissolved oxygen (O_2) concentrations within the Biosphere 2 coral reef biome over a 3-yr period (1 January 1997–1 January 2000), to calculate daily rates of gross production (P), community respiration (R), and net community production (NCP). P averaged 170 mmol O_2 m^{-2} d^{-1}, and R averaged 173 mmol O_2 m^{-2} d^{-1}, which yielded a mean NCP of only -3 mmol O_2 m^{-2} d^{-1}, or a difference of only 2%. This long-term balance between P and R reflects the closed-system design of the biome. The SD of P, however, was ± 56 mmol O_2 m^{-2} d^{-1}; that of R was ± 47 mmol O_2 m^{-2} d^{-1}; and that of NCP was ± 26 mmol O_2 m^{-2} d^{-1} or ± 15% of mean P. To better resolve the behavior of P, R, and NCP at different timescales, each of these time series were spectrally decomposed into four frequency bands that corresponded to four timescales: <1 week, 1 week–1 month, 1–3 months (subseasonal), and >3 months (seasonal to annual). At timescales >1 month, the variance of P was not different from the variance of R. At timescales of <1 month, the variance in P was significantly greater than the variance in R ($P < 0.01$). Furthermore, the correlation between changes in P and changes in R became weaker with decreasing timescale. We suggest that changes in P and R become well matched at timescales that coincide with the turnover of carbon by the dominant macroalgae within the biome (1–3 months). In addition, we conclude that measurements of NCP based on daily or weekly data sets are not good indicators of the long-term net metabolic performance of coral reefs.

Coral reefs are mosaics of autotrophic and heterotrophic communities that are often arranged to maximize consumption of produced organic matter (Odum and Odum 1955; Smith and Marsh 1973; Kinsey 1979; Crossland and Barnes 1983; Barnes and Devereux 1984). Consequently, it is suggested that spatial integration of local net production should lead to average rates of gross production (P) and community respiration (R) that are more balanced at larger spatial scales, P/R $\sim$ 1.0 (Kinsey 1985; Hatcher 1988, 1990; Crossland et al. 1991; Gattuso et al. 1998). Yet P and R change seasonally, doubling from winter to summer (Atkinson and Grigg 1984; Kinsey 1985). These seasonal changes appear to be independent of latitude and are likely caused by changes in temperature and incident light (Kinsey 1985). Little is known, however, about how well changes in P and R are coupled on timescales much shorter than seasonal variations (i.e., days to weeks). Are changes in R as tightly coupled with changes in P on short timescales (days to weeks) as they apparently are on seasonal timescales? If so, are rates of net community production (NCP) by reef communities no different from one time to the next and from one timescale to the next? In this study, to determine the temporal behavior of NCP, we analyzed temporal changes in P and R of a completely enclosed, self-sustained coral reef mesocosm at the Biosphere 2 Center.

The Biosphere 2 coral reef biome is an experimental, high-latitude, low-energy coral reef community in which accurate measurements of P, R, and NCP are made. Rates of P and R are similar to those found in other high-latitude, low-energy environments (Atkinson et al. 1999). The biome environment differs from natural, high-latitude reefs in that both temperature and flow conditions are tightly controlled, whereas only incident light varies according to local weather. The reef is completely closed with respect to the biogeochemical budgets of carbon, nitrogen, phosphorus, and trace metals. We monitored dissolved O_2 in this system for 3 yr, achieving a high-quality data set of daily rates of P, R, and NCP. The present study is an analysis of the relationships among P, R, and NCP within the reef mesocosm at different timescales.

Materials and Methods

Biosphere 2 reef biome—The Biosphere 2 (B2) Center is located $\sim$15 km north of Tucson, Arizona in the foothills

[1] Corresponding author (jfalter@soest.hawaii.edu).

Acknowledgments

We thank Heidi Barnett and Francesca Marubini for collecting data from the mesocosm and Mark Merrifield and Steve Smith for help with the analyses. This research was supported by University of Hawaii Sea Grant Program project numbers R/EL-1 and R/CR-1 as well as by the Biosphere 2 Corporation, Tucson, Arizona.

This is Hawaiian Institute of Marine Biology contribution 1116 and School of Ocean and Earth Science and Technology 5805.

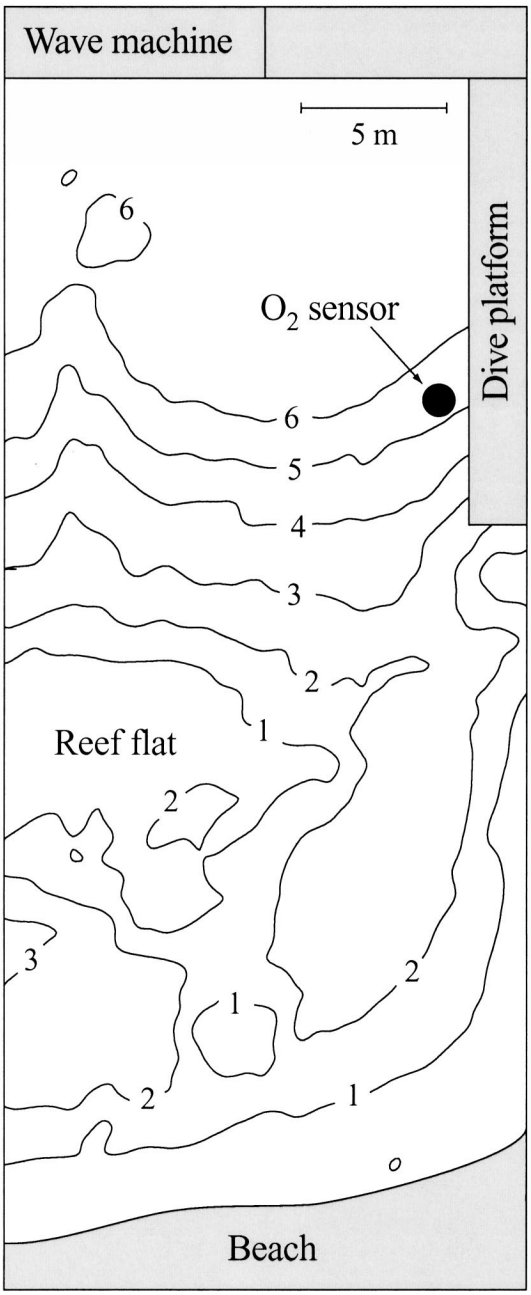

Fig. 1. Aerial view of the B2 coral reef biome. The depth of each contour is in meters.

of the Catalina mountains (32°34′N, 110°51′W). The B2 coral reef biome has a surface area of 711 m^2, a benthic surface area of ~850 m^2 including the walls, and a volume of 2,650 m^3 (Fig. 1). The biome is divided into four distinct zones: ocean, fore-reef, reef-flat, and shallow lagoon. Water depth ranges from 7 m in the ocean to 0.1 m at the shallowest part of the reef flat. The fore-reef, reef flat, and shallow lagoon cover a projected area of ~590 m^2. Waves of ~20–30 cm in height are created by a vacuum-driven wave generator whose outflow is located ~0.5 m below the water's surface, along one half of the south wall of the biome (Fig. 1). The waves impinge on the fore-reef, dissipate most of their energy on the reef-flat, and in the process help drive water exchange between the ocean and lagoon. This water exchange is further enhanced by pumping water from intakes located on the lagoon floor and underneath the dive platform to the bottom of the ocean. This forced flow is sent through heat exchangers that maintain nearly constant water temperatures within the biome at 26.5 ± 0.5°C. The mixing time of the ocean is ~1 h (Atkinson et al. 1999). Evaporative losses are compensated for by the introduction of low-nutrient fresh water filtered by reverse osmosis.

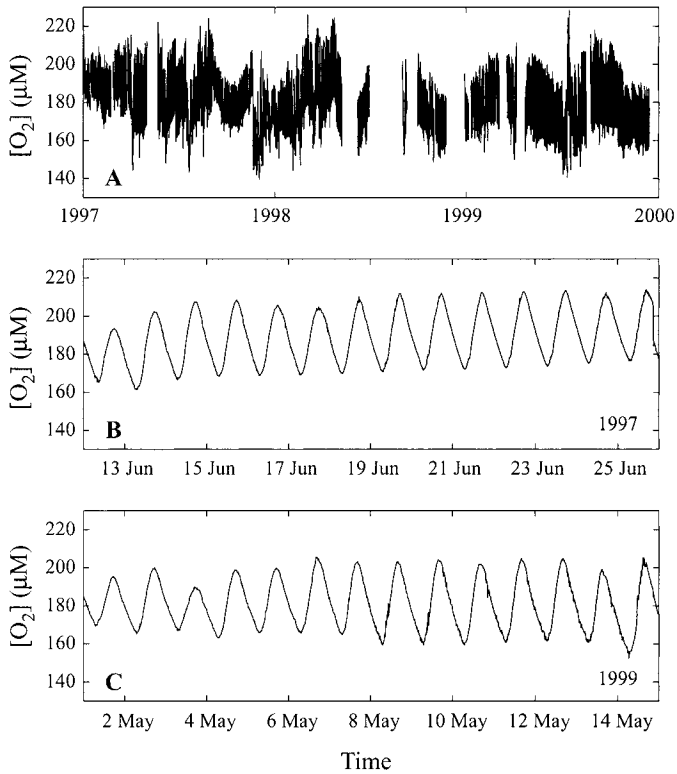

Fig. 2. (A) Concentration of dissolved O_2 versus time in the B2 reef biome for the period of 1 January 1997 through 31 December 1999. (B) Diel changes in dissolved O_2 as measured by the ENDECO pulsed O_2 sensor between 12 and 26 June 1997. (C) Diel changes in dissolved O_2 as measured by the Seabird O_2 sensor between 1 and 15 May 1999.

The benthic community within the B2 reef biome is dominated by both calcareous and noncalcareous macroalgae belonging to the families of chlorophyta, rhodophyta, and phaeophyta (see Atkinson et al. 1999 for a full description of the algal community). Although there is some coral growth within the biome, corals cover <2% of the benthic surface area. Grazing in the community is dominated primarily by meiofaunal amphipods and several hundred herbivorous fish of the family Acanthuridae. Incident light levels to the biome are relatively low in comparison with tropical reefs. Typical daily maxima of measured photosynthetically active radiation (PAR) irradiance at the reef flat (~0.5 m deep) range between 1,200 and 1,400 $\mu E\ m^{-2}\ s^{-1}$, or roughly three quarters the maximum PAR irradiances found in a lower latitude reef (1,500–2,000 $\mu E\ m^{-2}\ s^{-1}$ in

Table 1. Correlation coefficients (r^2) between changes in NP_{light} and R_{dark}, P and R, and P_2 and R_2. Correlations between NP_{light} and R_{dark} are provided assuming that rates of light respiration were zero (see Eqs. 3–5). P and R were calculated assuming that rates of light respiration were equal to rates of dark respiration. P_2 and R_2 were calculated assuming that rates of light respiration were double those of dark respiration. The number of degrees of freedom (*df*) for each decomposed time series is also provided.

Timescale	r^2 (NP_{light}, R_{dark})	r^2 (P, R)	r^2 (P_2, R_2)	*df*
<1 week	0.29	0.49	0.65	536
week–month	0.22	0.56	0.75	165
1–3 months	0.20	0.67	0.84	33
>3 months	0.44	0.89	0.96	17

Moorea, French Polynesia, 17°29′S, Gattuso et al. 1993, 1996), and the B2 space frame windows remove nearly all of the incident ultraviolet light. Nutrient levels within the biome are comparable with levels found on natural coral reefs with concentrations of NO_3^- (mean, 0.30 μM; max, 1.67; min, 0.02; $n = 190$), NH_4^+ (mean, 0.25 μM; max, 1.88; min, 0.02; $n = 190$), and Si (mean, 11.7 μM; max, 34.3; min, 2.9; $n = 190$) typical of those found in other reef environments, whereas concentrations of dissolved inorganic phosphate are relatively lower (mean, 0.040 μM; max, 0.44; min, undetectable; $n = 190$). Total alkalinity and total dissolved inorganic carbon have been manipulated in the biome to control carbonate (CO_3^{2-}) activities and CO_2 partial pressures (range in dissolved inorganic carbon, 1,800–2,100 μM; pCO_2, 200–700 μatm; and Ω_{arag}, 2.4–5.1; Langdon et al. 2000).

Dissolved oxygen measurements—Dissolved O_2 was monitored by use of both an ENDECO pulsed O_2 sensor (Lamont-Doherty) from January 1997 to September 1998 and a Seabird 22y YSI polaragraphic O_2 sensor (Seabird Electronics) from September 1998 to the present. Both sensors were deployed as part of a conductivity-temperature-depth package off the dive platform (Fig. 1). A total of 90% of the water in the biome is in the deep section, or ''ocean,'' and the biome is mixed within 1 h, so it is appropriate to monitor dissolved O_2 concentrations within this area. Measurements of sensor output were made every 15 min, whereas direct measurements of O_2 were determined via Winkler titration of three to five replicates taken twice daily. There was no systematic difference between each sensor's estimates of O_2 within the biome over a several-month period during which they were both deployed. The sensor membrane for the YSI probe was cleaned once a week and changed every 2 weeks. For the YSI probe, measurements of sensor output were regressed against all O_2 measurements between membrane changes; for the pulsed O_2 sensor, subsections of the sensor record were calibrated independently. The gaps of missing data can be attributed to periods of inadequate sensor performance and time for sensor repairs.

Estimates of P, R, and NCP—We define NCP to be net community production integrated over a 24-h period, (named

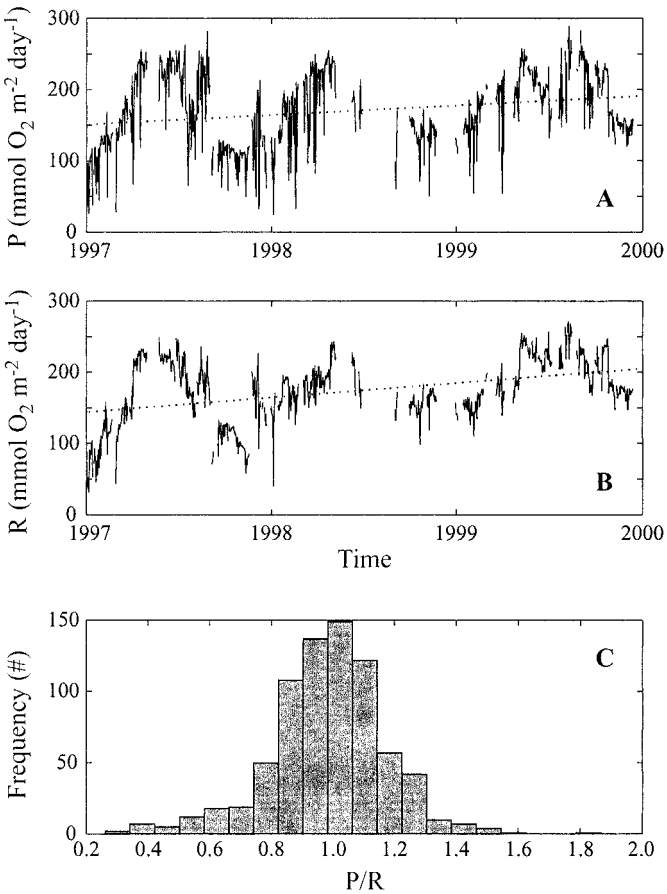

Fig. 3. (A) P of the B2 reef biome versus time for the period of 1 January 1997 through 31 December 1999 (slope of trend line, 0.037 mmol O^2 m^{-2} d^{-2}). (B) R in the B2 reef biome versus time for the period of 1 January 1997 through 31 December 1999 (slope of trend line, 0.056 mmol O^2 m^{-2} d^{-2}). P and R were calculated from diel O_2 under the assumption that rates of light respiration equaled rates of dark respiration. (C) Histogram of daily P : R ratios.

''E'' by Kinsey 1985). Net production (NP) is defined here as the instantaneous rate of net dissolved O_2 change and O_2 disequilibrium between the biome water and the B2 atmosphere according to

$$NP(t) = \left(\frac{1}{A_b}\right)\left[V\frac{d[O_2]}{dt} + \nu_{ex}A_s([O_2](t) - [O_2]_{sat})\right] \quad (1)$$

where the above variables are defined as follows:

$[O_2]$ measured dissolved oxygen concentration;
$[O_2]_{sat}$ concentration of dissolved oxygen in equilibrium with the atmosphere;
V volume of the ocean (2,650 m^3);
A_b surface area of bioactive benthos (850 m^2);
A_s surface area of the air-water interface (711 m^2);
ν_{ex} gas exchange coefficient (2.3 $\pm$ 0.4 m d^{-1}); and
t time in decimal days.

The gas exchange constant was measured specifically for O_2 six times between September 1995 and April 2000. The air-sea gas exchange coefficient should be relatively constant, given the nearly constant wave conditions within the

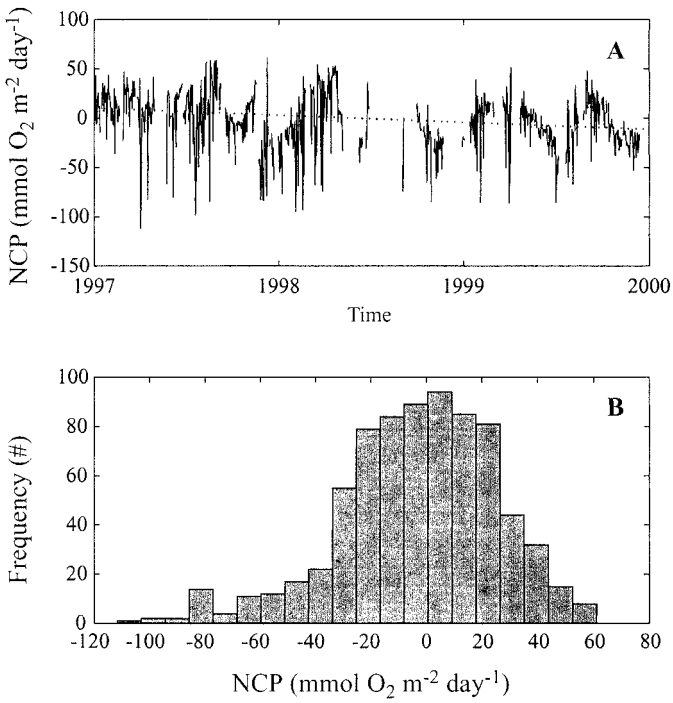

Fig. 4. (A) NCP in the B2 reef biome versus time for the period of 1 January 1997 through 31 December 1999 (slope of trend line, −0.020 mmol O^2 m^{-2} d^{-2}). (B) Histogram of daily NCP values.

ocean and the absence of wind within the biome (Wanninkhof 1992). The equilibrium concentration of O_2 was calculated by use of the O_2 solubility equation of Weiss (1970). The partial pressure of O_2 in the B2 atmosphere was estimated by use of the mean annual atmospheric pressure of 887.6 mBar (n = 73,282; SD, 3.9) and a salinity of 35.5 psu. Metabolic rates were normalized to total benthic surface area (850 m^2), which included surfaces at 7 m depth and on vertical walls. These surfaces receive less light than shallower areas of the biome (590 m^2) and thus may lead to underestimates of actual community metabolic rates. The normalization to 850 m^2, however, does not change relationships among P, R, and NCP.

Equation 1 can be integrated to estimate net production over a known time interval.

$$\int_{t_1}^{t_2} NP(t)\,dt = \left(\frac{1}{A_b}\right)\left[V([O_2]_{t_2} - [O_2]_{t_1}) + \nu_{ex} A_s \int_{t_1}^{t_2} ([O_2] - [O_2]_{sat})\,dt\right] \quad (2)$$

Integrating $NP(t)$ from sunrise to sunset yields the amount of net production that occurs over the daylight hours (NP_{light}), and integration of $NP(t)$ from sunset to sunrise yields the amount of dark respiration (R_{dark}). Sunrise and sunset times for the B2 ocean were estimated by determining when PAR irradiance levels on the reef crest rose above 10 μE m^2 s^{-1} for at least 1 h (sunrise) and fell below 10 μE m^2 s^{-1} for at least 1 h (sunset). These criteria were established to distinguish transient spikes in the light record from systematic shifts at low light levels. Sunset times determined by use of these criteria were within ±12 min of sunset times determined at nearby Tucson airport (http://aa.usno.navy.mil/data/docs/RS_OneYear.html), whereas sunrise times were 23 (±7) min later. The difference in sunrise times can be attributed to the location of Catalina mountains, which sit directly to the east of the B2. PAR irradiance was measured by use of a LICOR LI-193SA Spherical Quantum Sensor (LICOR).

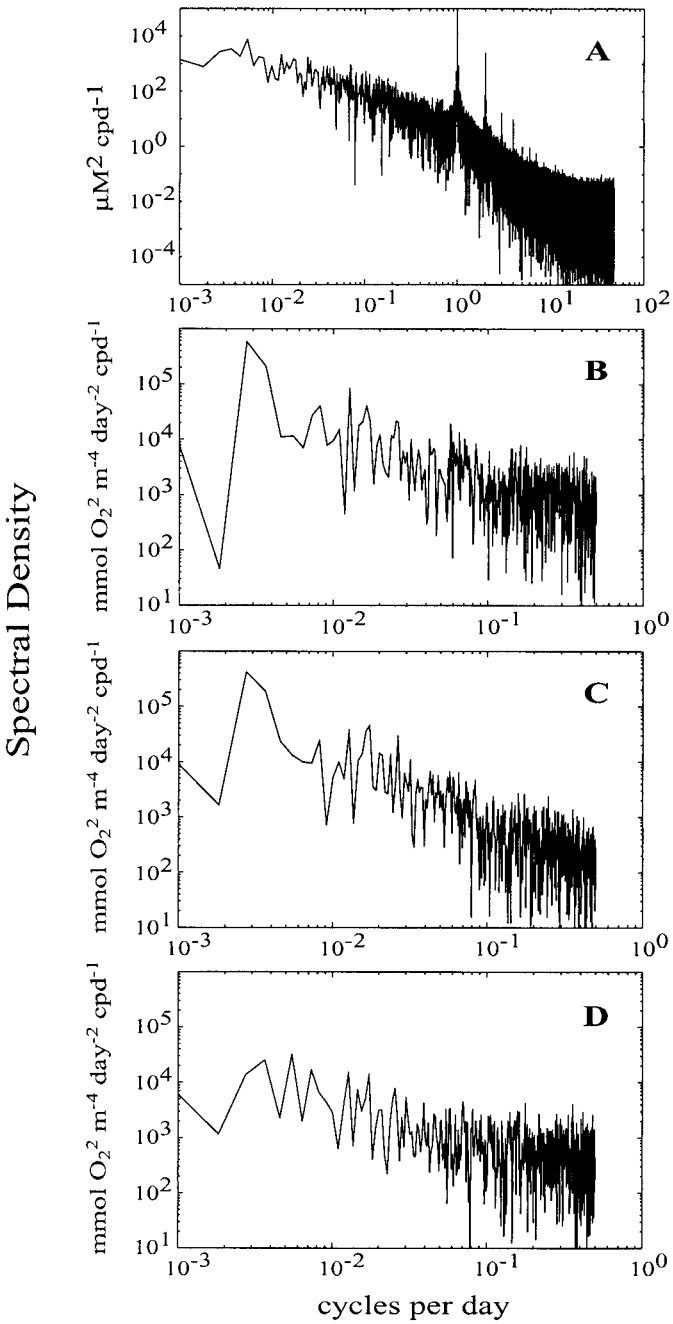

Fig. 5. Power spectral densities representing variability of (A) O_2, (B) P, (C) R, and (D) NCP.

Gaps in the O_2 record of <3 h in duration were interpolated from the surrounding data with third-order polynomi-

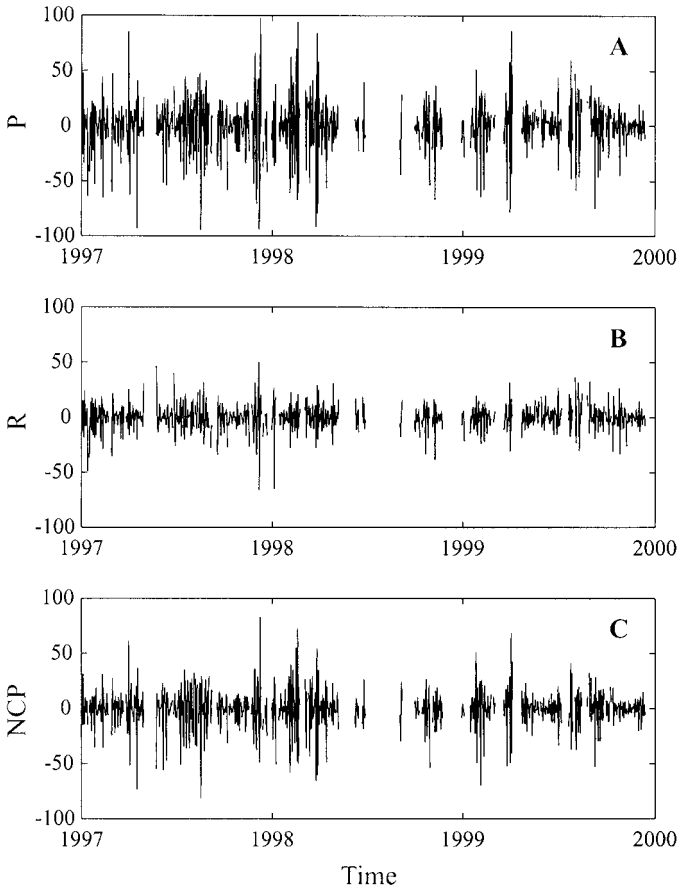

Fig. 6. Changes in (A) P, (B) R, and (C) NCP at timescales of <1 week. Y-axis values for all plots are in mmol O_2 m^{-2} d^{-1}.

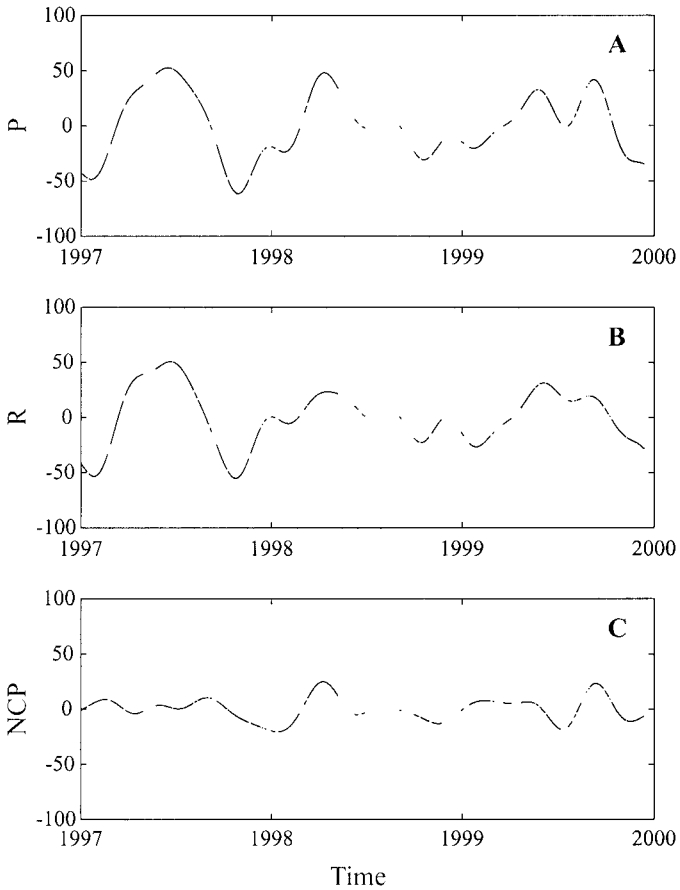

Fig. 7. Changes in (A) P, (B) R, and (C) NCP at timescales >3 months. Y-axis values for all plots are in mmol O_2 m^{-2} d^{-1}.

als, to reflect the quasisinusoidal oscillations in diel O_2 concentrations; such corrections were applied to <10% of the data. Estimates of P and R were not made on days in which there were gaps >3 h in the original O_2 record.

P and R were calculated as follows:

$$P = NP_{\text{light}} + R_{\text{light}} \tag{3}$$

$$R = R_{\text{light}} + R_{\text{dark}} \tag{4}$$

where R_{light} is proportional to R_{dark} by the length of day (τ_{day}) divided by the length of night (τ_{night}) (Eq. 5).

$$R_{\text{light}} = \frac{\tau_{\text{day}}}{\tau_{\text{night}}} R_{\text{dark}} \tag{5}$$

The assumption that rates of light respiration are equivalent to rates of dark respiration has been customary for all estimates of P and R in coral reefs. This assumption inherently adds a positive covariance between P and R and will be considered in the discussion section. NCP was determined by direct integration of $NP(t)$ from sunrise on one day to sunrise on the next. Estimates of NP_{light}, R_{dark}, and NCP were performed by use of a trapezoidal integration scheme.

Spectral decomposition—The O_2, P, R, and NCP time series were each transformed into the frequency domain to evaluate their spectral characteristics. All time series were linearly detrended and had their mean values subtracted before spectral decomposition (Bendat and Piersol 1986). Gaps in the de-meaned, detrended time series were replaced with zeros so as not to contribute to the calculation of the discrete Fourier transform. To better examine the relationship among P, R, and NCP on different timescales, each of these time series were spectrally decomposed into four frequency bands that corresponded to four different timescales: <1 week (2–7 d), 1 week–1 month (7–30 d), subseasonal (1–3 months), and seasonal to annual (>3 months). These frequency bands were chosen to both resolve the temporal relationship between P and R at timescales of interest while still having enough information to characterize the relationships among P, R, and NCP within each frequency band or set of timescales. To seek a finer resolution of how these relationships vary at different timescales would only lead to less robust interpretations, given the limited number of data points in each of the time series (751). The total number of degrees of freedom (n_T = 751) was taken as the number of days out of the 3-yr period for which there were reliable estimates of P, R, and NCP. This number was used in computing the variance of each decomposed time series so that they would be properly scaled in terms of their amplitudes. However, the 95% confidence intervals for each variance estimate were made with the actual number of degrees of freedom used in reconstructing the decomposed time series (Table 1). The

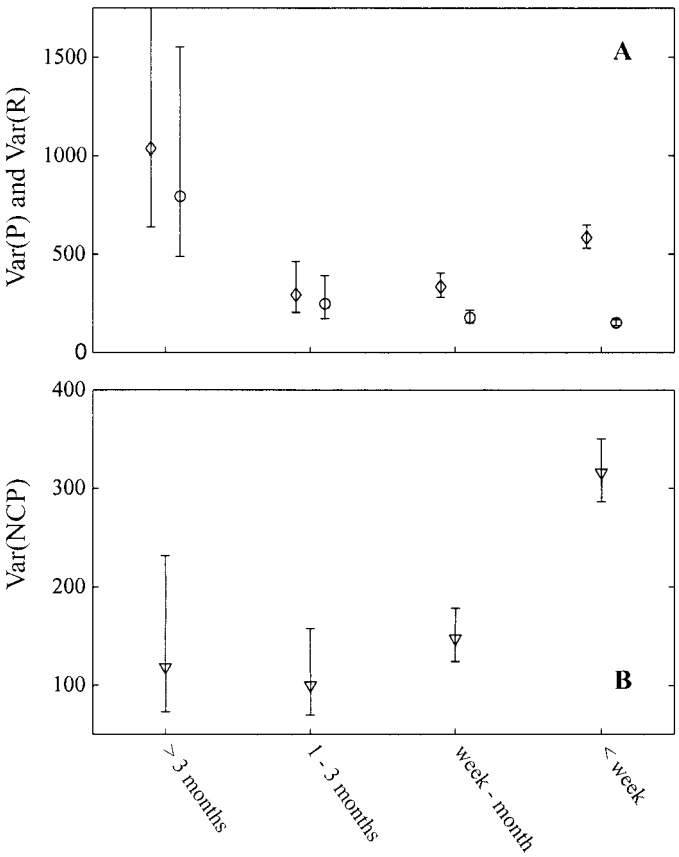

Fig. 8. (A) Variances of P (diamonds) and R (circles), with their 95% confidence limits for each set of timescales. The X-axis for each plot has been shifted slightly for clarification. (B) Variances of NCP, along with their 95% confidence limits at each set of timescales.

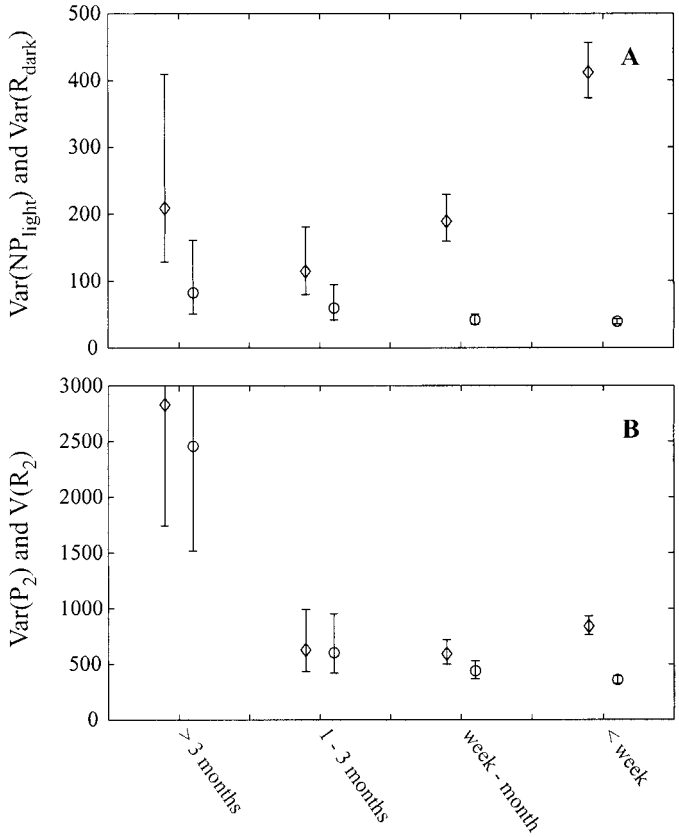

Fig. 9. (A) The variances of NP_{light} (diamonds) and R_{dark} (circles), with their 95% confidence limits for each set of timescales. NP_{light} and R_{dark} are assumed to be independent variables and R_{light} is assumed to be 0. The X-axis for each plot has been shifted slightly for clarification. (B) The variances of P and R with their 95% confidence limits, when rates of light respiration are assumed to be twice that of rates of dark respiration. Note the increased variance between (A) and (B). The X-axis for each plot has been slightly shifted for clarification.

greater degrees of freedom for the shorter timescales reflect the larger number of frequency components used to define their respective time series and is a direct consequence of transforming information between the frequency and time domains.

Results

Time series—Diurnal changes in dissolved O_2 were typically 20–40 μM over the 3-yr period (Fig. 2). The mean error in sensor-estimated O_2 was 1.5 μM. The mean O_2 (180.0 μM) over the time series was only slightly lower than the mean O_2 saturation (180.6 μM). Spatial variability in O_2 between the lagoon and deep ocean were typically $\sim$10 μM, which represents a $\sim$1% error in the total mass of O_2 in the biome.

Estimates of P, R, and NCP were available for 751 of the 1,095 d (69%) over the 3-yr period. P averaged 170 mmol O_2 m^{-2} d^{-1}, with a range of 25–290 mmol O_2 m^{-2} d^{-1}; and R averaged 173 mmol O_2 m^{-2} d^{-1}, with a range of 32–272 mmol O_2 m^{-2} d^{-1}. As had been expected, P and R were well correlated ($r^2 = 0.72$, $n = 751$, $P < 0.01$) and showed a strong seasonal dependency (Fig. 3A–C). The magnitude of changes in P and R (SD) were 33% ($\pm$55 mmol O_2 m^{-2} d^{-1}) and 27% ($\pm$47 mmol O_2 m^{-2} d^{-1}) of their respective means. Both P and R increased significantly with time, which indicates an overall increase in the metabolism of the biome ($P < 0.01$). The average error in estimated P and R due to uncertainties in dissolved O_2 concentration, temperature, salinity, and O_2 partial pressure inside the B2 atmosphere was 9 mmol O_2 m^{-2} d^{-1} for both time series. Error in the values of P, R, and NCP due to uncertainty in the value of the gas-exchange coefficient averaged less than $\pm$1 mmol O_2 m^{-2} d^{-1}. Daily P to R ratios averaged 0.99, with $\sim$80% of the values lying between 0.8 and 1.2 (Fig. 3C). Both P and R increased with time, and their slopes were significantly >0 ($P < 0.05$). NCP ranged between $-$112 and 61 mmol O_2 m^{-2} d^{-1}, with a mean value of $-$3 mmol O_2 m^{-2} d^{-1}, and showed a decreasing trend over time ($P < 0.05$, Fig. 4A). The average error in estimates of NCP was 7 mmol O_2 m^{-2} d^{-1}. The SD of NCP was $\pm$26 mmol O_2 m^{-2} d^{-1} or $\sim$15% of mean P or R. Over 80% of all NCP values were within $\pm$38 mmol O_2 m^{-2} d^{-1} or $\pm$20% of mean P (Fig. 4B).

Spectral decomposition—Spectral representation of O_2 data, as had been expected, showed the strong diurnal signal

(1 cpd), with increasing spectral density at lower frequencies or longer timescales (Fig. 5A). Spectral representation of P, R, and NCP time series indicate that most of the energy or variability lies within the lower frequencies (Fig. 5B–D). Examples of the original P, R, and NCP time series decomposed to changes that occurred on timescales of <1 week and <1 month are provided in Figs. 6 and 7. The correlations between changes in P and changes in R were significantly positive at all timescales ($P < 0.01$) and were weakest at the shortest timescales (Table 1).

The variance of P decreased from a high at the longest timescales to a minimum at 1–3 months and then increased at the shortest timescales. The variance of R steadily decreased from a maximum at timescales >3 months to a low at timescales of <1 week (Fig. 8). The variances in both P and R at the longest timescales were significantly greater than the variance for all other timescales ($P < 0.025$); nearly half of the variance of both P and R were carried at these timescales. The variance of R was significantly lower than the variance of P at timescales of <1 month, but these variances were not significantly different at timescales >1 month ($P < 0.0001$). Surprisingly, the variance in NCP at timescales of <1 week was significantly greater than the variance in NCP at all other timescales considered ($P < 0.05$).

Discussion

In the present article, we have estimated the true values of P and R by partitioning these two separate processes into NP_{light}, R_{dark}, and R_{light} (Eqs. 3–5). On the basis of these definitions, correlations between P and R are affected by how R_{light} is approximated. Even if R_{light} was assumed to be zero (Eqs. 3 and 4), NP_{light} and R_{dark} are significantly correlated at all timescales and are most highly correlated at the longest timescale (Table 1, $P < 0.01$). The pattern of the variance in NP_{light} and R_{dark} at different timescales is similar to that of P and R, with higher variances of NP_{light} than R_{dark} at timescales <1 month (compare Fig. 9A with Fig. 8A). Reasonable estimates of R_{light} will not greatly affect our interpretation of the temporal relationships between true P and true R. For example, if rates of light respiration were twice that of dark respiration, correlations between P and R improve slightly (10%–30%, Table 1), but the disparity between their variances at shorter timescales still remains (Fig. 9B).

Light must be the dominant factor controlling changes in P for two reasons: (1) the B2 biome has constant temperature and no external sources of carbon or nutrients, and (2) PAR and P were significantly correlated ($P < 0.001$, $r^2 = 0.62$, $n = 85$). In turn, seasonal changes in R must respond to seasonal changes in P because (1) P and R (or NP_{light} and R_{dark}) were most highly correlated at seasonal timescales and (2) R was not correlated to biomass in the B2 coral reef; R decreased from August 1999–December 1999, whereas algal biomass increased (V. Coelho and K. Fitzsimmons unpubl. data).

There is a component of R that responds to short-term changes in P, because NP_{light} and R_{dark} were significantly correlated even at timescales of <1 week. This rapid-response component probably represents an organic photosynthate pool that is respired by autotrophs. Nonetheless, variances of P and R are similar in magnitude at timescales >1 month and, along with better correlations, indicate a much greater balance between changes in P and changes in R at longer timescales. These results suggest that most organic carbon turnover within the mesocosm occurs at timescales that are closely related to the turnover time of the dominant macroalgae (~1 month).

We conclude that daily measurements of NCP are not indicative of system performance and can vary ±15% from the average value. We expect this variability in NCP to be even greater in natural coral reefs, where changes in nutrient and carbon inputs may alter responses of the different carbon pools. Understanding relationships between the autotrophic and heterotrophic components of reefs will require much longer temporal integrations than have been previously used.

References

ATKINSON, M. J., AND OTHERS. 1999. The Biosphere 2 coral reef biome. Ecol. Engineering **13:** 147–171.

———, AND R. W. GRIGG. 1984. Model of a coral reef ecosystem: II. gross and net benthic primary production at French Frigate Shoals, Hawaii. Coral Reefs **3:** 13–22.

BARNES, D. J., AND M. J. DEVEREUX. 1984. Productivity and calcification on a coral reef: A survey using pH and oxygen electrode techniques. J. Exp. Mar. Biol. Ecol. **79:** 213–231.

BENDAT, J. S., AND A. G. PIERSOL. 1986. Random data: Analysis and measurement procedures, 2nd ed. Wiley.

CROSSLAND, C. J., AND D. J. BARNES. 1983. Dissolved nutrients and organic particulates in water flowing over coral reefs at Lizard Island. Aust. J. Mar. Freshw. Res. **34:** 835–844.

———, B. G. HATCHER, AND S. V. SMITH. 1991. Role of coral reefs in global production. Coral Reefs **10:** 55–64.

HATCHER, B. G. 1988. The primary productivity of coral reefs: A beggar's banquet. Trends Ecol. Evol. **3:** 106–111.

———. 1990. Coral reef primary productivity: A hierarchy of pattern and process. Trends Ecol. Evol. **5:** 149–155.

———, M. FRANKIGNOULLE, AND R. WOLLAST. 1998. Carbon and carbonate metabolism in coastal aquatic ecosystems. Annu. Rev. Ecol. Syst. **29:** 405–434.

GATTUSO, J.-P., M. PINCHON, B. DELESALLE, AND M. FRANKIGNOULLE. 1993. Community metabolism and air-sea CO_2 fluxes in a coral reef ecosystem (Moorea, French Polynesia). Mar. Ecol. Prog. Ser. **96:** 259–267.

———, ———, ———, C. CANON, AND M. FRANKIGNOULLE. 1996. Carbon fluxes in coral reefs. I. Lagrangian measurement of community metabolism and resulting air-sea CO_2 disequilibrium. Mar. Ecol. Prog. Ser. **145:** 109–121.

KINSEY, D. W. 1979. Carbon accumulation and turnover by coral reefs. Ph.D. dissertation, Univ. of Hawaii.

———. 1985. Metabolism, calcification and carbon production 1: System level studies. Proc. 5th Int. Coral Reef Congr. **4:** 505–526.

LANGDON, C. L., AND OTHERS. 2000. Effect of calcium carbonate

saturation state on the calcification rate of an experimental coral reef. Global Geochem. Cycles **14:** 639–654.

ODUM, H. T., AND E. P. ODUM. 1955. Trophic structure and productivity of a windward coral reef community on windward Eniwetok Atoll. Ecol. Monogr. **25:** 291–320.

SMITH, S. V., AND J. A. MARSH. 1973. Organic carbon production on the windward reef flat of Eniwetok Atoll. Limnol. Oceanogr. **18:** 953–961.

WANNINKHOF, R. 1992. Relationship between wind speed and gas exchange over the ocean. J. Geophys. Res. **97:** 7373–7382.

WEISS, R. F. 1970. The solubility of nitrogen, oxygen, and argon in water and seawater. Deep-Sea Res. **17:** 721–735.

Received: 2 January 2001
Accepted: 9 July 2001
Amended: 31 July 2001